



On the influence of gravel bed dynamics on velocity power spectra

Arvind Singh,¹ Fernando Porté-Agel,¹ and Efi Foufoula-Georgiou¹

Received 7 May 2009; revised 21 October 2009; accepted 24 November 2009; published 24 April 2010.

[1] A series of flume experiments were conducted to study the effect of bed form dynamics on the flow over a gravel bed comprising a wide distribution of grain sizes. Instantaneous high-frequency streamwise flow velocities were sampled using an acoustic Doppler velocimeter at a frequency of 200 Hz, while the simultaneous bed elevations were sampled using sonar transducers at a frequency of 0.2 Hz for a duration of 20 h. Spectral analysis of the measured velocity fluctuations reveals the existence of two distinct power law scaling regimes. At high frequencies, an inertial subrange of turbulence with $\sim -5/3$ Kolmogorov scaling is observed. At low frequencies, another scaling regime with spectral slope of about -1.1 is found. We interpret this range as the signature of the evolving multiscale bed topography on the near-bed velocity fluctuations. The two scaling ranges are separated by a spectral gap, i.e., a range of intermediate scales with no additional energy contribution. The high-frequency limit of the spectral gap corresponds to the integral scale of turbulence. The low-frequency end of the gap corresponds to the scale of the smallest bed forms identified by the velocity sensor, which depends on the position of the sensor. Our results also show that the temporal scales of the largest bed forms can be potentially identified from spectral analysis of low-resolution velocity measurements collected near the channel bed.

Citation: Singh, A., F. Porté-Agel, and E. Foufoula-Georgiou (2010), On the influence of gravel bed dynamics on velocity power spectra, *Water Resour. Res.*, 46, W04509, doi:10.1029/2009WR008190.

1. Introduction

[2] Measurement of turbulent flow structures in a gravel bedded environment has received considerable attention in the past few decades; yet, there is still debate about the origin and development of these flow structures and, in turn, their influence on the bed surface itself [Wiberg and Smith, 1991; Dinehart, 1992; Robert *et al.*, 1992; Buffin-Bélanger and Roy, 1998; Lacey and Roy, 2007; Hardy *et al.*, 2009]. It has been suggested that the initiation of gravel movement is strongly influenced by large transient coherent flow structures with time scales of about 1–10 s which are superimposed on the more random small-scale turbulence [Drake *et al.*, 1988; Kirkbride, 1993; Kirkbride and McLelland, 1994; Kirkbride and Fergusson, 1995; Lamarre and Roy, 2005]. Over a rough boundary, such as in a gravel bedded channel, friction created by individual gravel particles or clusters of particles (i.e., microtopography as well as bed forms) retards the flow velocity, but the effect diminishes with increasing height above the bed [Lacey and Roy, 2007, 2008]. This surface roughness creates near-bed turbulence which is responsible for entrainment of particles predominantly linked to sweeps, bursts and larger coherent structures [Robert *et al.*, 1992; Best, 1993; Robert *et al.*, 1993; Lamarre and Roy, 2005; Schmeeckle *et al.*, 2007; Hardy *et*

al., 2009]. These large-scale coherent flow structures are a key component of turbulent boundary layers and scale with the flow depth, h [Roy *et al.*, 2004]. In a mobile gravel bed the size of these macroturbulent flow structures is found to scale with h in the vertical direction and 2 to 12 times h in the horizontal direction [Shvidchenko and Pender, 2001; Roy *et al.*, 2004]. The downstream motion of these flow structures may cause quasiperiodic fluctuations of the local flow velocity components and could lead to the development of troughs and ridges on the mobile bed, inducing bed particle destabilization (sediment transport). Imamoto and Ishigaki [1986a, 1986b] investigated the turbulent flow structure over smooth and rough immobile beds and detected the existence of upwelling and downwelling circular fluid motion over the entire flow depth. They found that both the lateral and the longitudinal integral scale of fluid motion was about $2h$. Yalin [1992] hypothesized that the macroturbulent structures are closely linked to the bursting phenomena in boundary layers and do not originate in their full size ($\sim h$). According to Yalin [1992] turbulent eddies are generated near the bed surface as a result of bursts with sizes much smaller than h , then grow until their size becomes approximately equal to h ; they are then destroyed, prompting the generation of new smaller eddies, and so on. The complete cycle of the eddies' formation, evolution, and destruction occurs over a distance of $\sim 6h$.

[3] In spite of the important role that these macroturbulent structures could play in the dynamics of rivers, there is no model that relates the interaction of turbulent flow structures to bed topography and sediment transport. This is partly due to the unavailability of long-reliable records of turbulent

¹Department of Civil Engineering, St. Anthony Falls Laboratory and National Center for Earth-Surface Dynamics, University of Minnesota, Minneapolis, Minnesota, USA.

data sampled at high resolution and partly due to the presence of complex bed topography varying spatially and temporally in a gravel bedded channel [Paiement-Paradis et al., 2003; Marquis and Roy, 2006]. In particular, little is known about how the relatively slow evolution of moving multiscale topography can affect the scaling properties (e.g., spectral density) of the velocity field at different positions in the flow. For instance, Dinehart [1999] associated the presence of large-scale/low-frequency fluctuations of velocity, obtained from long-velocity records, to migrating bed forms in gravel bed rivers. In a previous study Dinehart [1989] documented the passage of bed forms at periods ranging from 2 to 5 min that corresponds with velocity fluctuations. In a recent study Nikora [2008] suggested that the currently used three-range spectral model (production range, inertial subrange and dissipation range) for gravel bed rivers should be further refined by adding an additional range, leading to a model that consists of four ranges of scales with different spectral behavior and should be tested with field and experimental observations. However, to resolve the potential differences in velocity spectra, for example, between fixed and weakly mobile gravel beds, much longer velocity records would be required [Nikora and Goring, 2000].

[4] Unlike the situation in river flows, a considerable amount of work has been performed in atmospheric boundary layer flows toward characterizing and isolating the signature of relatively slow (synoptic scale, mesoscale) variability from that of the turbulence (for examples, see Van Der Hoven [1957], Fiedler and Panofsky [1970], and Smedman-Högström and Högström [1975]). In a classical work, Van Der Hoven [1957] showed a marked spectral gap between mesoscale (synoptic) and microscale (turbulent) flow variability in the analysis of large-range spectrum of horizontal wind velocity. Since then, several investigators have confirmed the existence of a spectral gap in the spectra of horizontal wind velocity over land. Hess and Clarke [1973] also showed a tendency for a gap in the spectra of wind velocity measured at different heights between the surface layer and free atmosphere.

[5] In this paper we use simultaneous high-resolution long time series of bed elevations and velocity fluctuations along with longitudinal transects of bed profile measured over a gravel bedded experimental channel to quantify the multiscale variability of both flow structures and bed structures. Our results show the signature of bed structures on the near-bed velocity fluctuations and point to the potential of using relatively low-frequency measurements of velocity in the field to detect time scale of bed topography in real rivers.

2. Experimental Setup and Data Analyzed

[6] Experiments were conducted in the Main Channel facility at St. Anthony Falls Laboratory, University of Minnesota. These experiments were the followup of previous experiments conducted in spring of 2006 known as StreamLab06 [Wilcock et al., 2008]. StreamLab06 was an 11 month multidisciplinary laboratory channel study focused on various aspects of ecogeomorphology in gravel bed streams. Five separate projects were conducted as part of StreamLab06, while all the studies shared the same sediment

and general experimental configuration. The extensive data set collected in these experiments includes hydraulic conditions (discharge, water slope, bed slope, depth average velocity, and flow field), morphological conditions (bed topography, bar locations and shapes, photo images of the bed), sediment transport characterization (continuous sediment flux, recirculation grain size information), water chemistry (temperature, dissolved oxygen, nutrient concentrations) and biological conditions (heterotrophic respiration, biomass accumulation, nutrient processing rates). For the experiments presented here (which we call Streamlab08), we focus on flow field and spatiotemporal bed topography for the discharges of 2000 L/s and 2800 L/s.

[7] The Main Channel is a 55 m long, 2.74 m wide channel with a maximum depth of 1.8 m and maximum discharge capacity of 8000 L/s (Figure 1). It is a partially sediment recirculating channel while the water flows through the channel without recirculation. The sediment recirculation system is capable of entraining and recirculating particles up to 76 mm in size. The recirculation system's intake is in the bed trap below the weigh pan system, where a horizontal auger, driven by a variable-speed motor, spans the full width of the channel. The rotating auger conveys sediments accumulated from weigh pan dumps toward an outlet recessed in the right side of the flume and into the recirculation pump (dredging pump) intake. The recirculation auger speed was adjusted manually every 30 min to maintain a constant elevation of sediment in the auger hopper and to continuously transport sediment through the recirculation pipe. This procedure avoided sending large pulses of sediment through the pipe each time a weigh pan dumped. Intake of the water in the channel was directly from the Mississippi River.

[8] The bed of the channel was composed of a mixture of gravel (median particle size diameter, $d_{50} = 11.3$ mm) and sand (median particle size diameter, $d_{50} = 1$ mm). It is fluvial in nature. A total of 15% sand was added to the gravel. The final grain size distribution obtained after mixing the sediments had a $d_{50} = 7.7$ mm, $d_{16} = 2.2$ mm and $d_{84} = 21.2$ mm. The mean specific density of sediment of all size fractions was ~ 2.65 . The thickness of the bed at the start of the run was approximately 0.45 m. Figure 2 shows the patches of bed surface obtained at the end of the run for a discharge of 2000 L/s (Figure 2a) and 2800 L/s (Figure 2b).

[9] Prior to data collection a constant water discharge, Q , was fed into the channel to achieve quasi-dynamic equilibrium in transport and slope adjustment for both water surface and bed. Sediment transport rates were measured simultaneously during the entire course of the run. Determination of the dynamic equilibrium state was evaluated by checking the stability of the 60 min average total sediment flux at the downstream end of the test section. Using the pan accumulation data, the acquisition software computed a 60 min mean of sediment flux in all five pans. Dynamic equilibrium was reached when variation in this value became negligible. In other words, when the average of the previous 60 min of instantaneous flux values computed from the pan data stabilized, we determined the channel to be in dynamic equilibrium and proceeded with formal data collection and sampling. After attaining equilibrium, experiments ran for approximately 20 h. (More details about the experimental setup can be found in the work by Singh et al. [2009a, 2009b].)

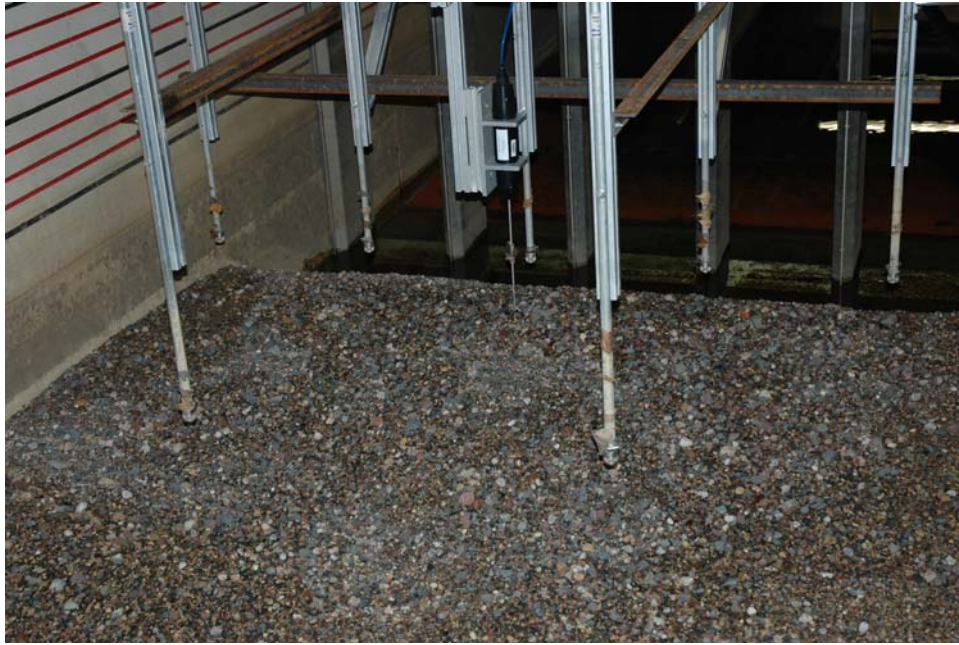


Figure 1. Experimental channel facility at St. Anthony Falls Laboratory, University of Minnesota, showing the locations of ADV and the sonar at the downstream end of the channel. A total of seven submersible sonars were deployed. In this study the data collected from the ADV and the sonar (located 15 cm downstream of ADV) along the centerline of the channel (see also schematic in Figure 3) are used. The direction of the flow is from the bottom to the top of the photograph.

[10] The data presented here are the velocity fluctuations (in the flow direction), simultaneous temporal bed elevation collected at the downstream end, and the longitudinal transects of bed profile, measured along the centerline of the channel. The continuous velocity fluctuations were measured using an acoustic Doppler velocimeter (ADV) at an approximate distance of 15 cm above the mean bed level. Relative heights, the ratio between D_p (distance of velocity probe from mean bed level) and D (average depth of flow), were computed to be 0.23 and 0.29 for the discharge of 2000 L/s and 2800 L/s, respectively (see Table 1). Nortek

Vectrino⁺ ADV was used for this study. The ADV was mounted 20 cm upstream of the centrally located bed sonar (sonar 3, see Figure 3) and could measure 3D water velocity with a sampling frequency of 200 Hz, and a precision of ± 1 mm/s.

[11] For the bed elevation measurements, submersible sonar transducers of 2.5 cm diameter were deployed 0.3 m (on an average) below the water surface. These sonar transducers were mounted to the end of rigid 1.5 cm steel tubes and directed perpendicular to the bed. The transducers collected continuous temporal bed elevation information



Figure 2. Photograph of bed surface at the end of the flow for the discharges of (a) 2000 L/s and (b) 2800 L/s. The direction of flow in both cases is from the top to the bottom of the photographs.

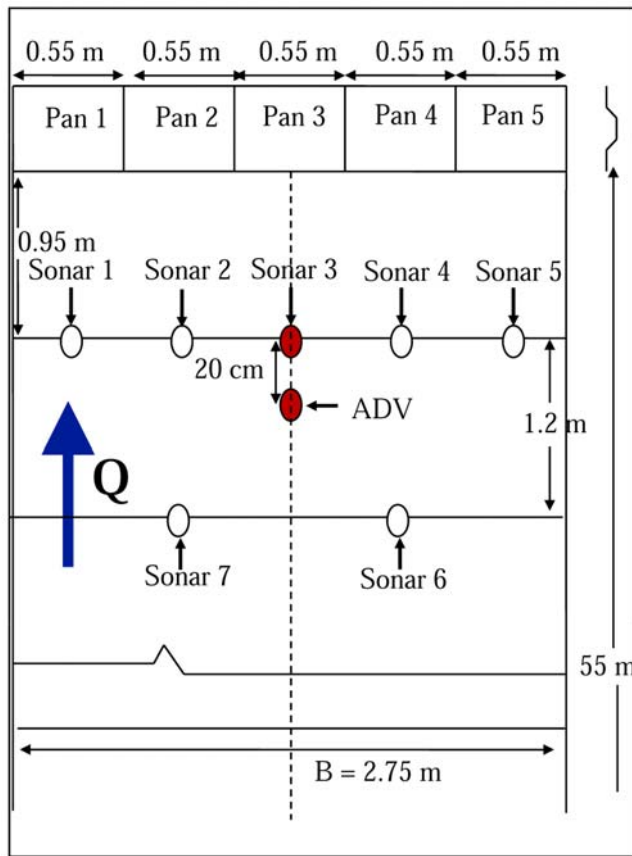


Figure 3. Schematic of experimental setup showing the locations of sonars (used for measuring temporal bed elevation) and the ADV (used for measuring velocity fluctuations) at the downstream end of the channel. Note that the solid dots represent the measurement locations of temporal bed elevations ($h(t)$) and velocity ($v(t)$) used in this study. The dashed line represents the centerline of the channel.

upstream of each weigh pan. The sampling interval of bed elevation measurements was 5 s with a vertical precision of 1 mm. Figures 1 and 3 (schematic) show the setup of ADV and the sonar placed at the downstream end of the channel. Measurements were taken over a range of discharges corresponding to different bed shear stresses. Bed shear stress is often characterized in terms of the dimensionless Shields stress, τ_b^* . For steady, uniform flow it may be approximated as

$$\tau_b^* = \frac{h_R S}{R d_{50}}, \quad (1)$$

where h_R and S are the hydraulic radius and channel slope, respectively, and $R = 1.65$ is the relative submerged density of silica. Here we report the data collected at discharges of 2000 L/s and 2800 L/s corresponding to Shields stress of 0.058 and 0.099, respectively (for details about the hydraulic conditions see Table 1). (Note that for computing Reynolds number and Froude number, kinematic viscosity of water (ν), and acceleration due to gravity (g), were taken as $1 \times 10^{-6} \text{ m}^2/\text{s}$, and 9.81 m/s^2 , respectively.) Critical Shields stress (τ_c^*) was assumed to be 0.03 as suggested by *Buffington and Montgomery* [1997] and references therein. Figures 4a and 4c show the time series of velocity fluctuations and the corresponding bed elevations for discharges of 2000 L/s and 2800 L/s, respectively, collected for the duration of 20 h.

[12] For the longitudinal bed profiles a three-axis positionable data acquisition (DAQ) carriage was used. This DAQ was designed, fabricated, and installed at St. Anthony Falls Laboratory. The DAQ carriage was capable of traversing the entire 55×2.74 meter test section and could position probes to within 1 mm in all three axes. Streamwise travel speeds of DAQ could be set up to 2 m/s. The DAQ carriage was controlled by a backbone computer that also served as the master time clock for all data collection in the study.

[13] Because the data were collected in the fall, there were some leaves floating in the channel which might have resulted in spikes in the velocity and bed elevation data. Even though the amount of spurious spikes in the data (0.81 percent for 2000 L/s and 0.79 percent for 2800 L/s) was found to be very small, these were removed as part of the data treatment for erroneous measurements using the methodology described by *Parshah et al.* [2010]. *Parshah et al.* [2010] used a modified version of the universal phase space thresholding technique proposed by *Goring and Nikora* [2002] for detecting the spikes and subsequently replacing them by the last valid data points with the sample-and-hold technique [*Adrian and Yao*, 1987].

3. Spectral Analysis Results

[14] Power spectral density (PSD) is a commonly used tool to measure the distribution of energy (variance) in the signal across frequencies (or scales). In other words, it shows at which scales the contribution to the signal variance are strong and at which scales contribution to the signal variance are weak. For a signal $X(t)$, the power spectral density is given by

$$\Phi(\omega) = \frac{1}{2\pi} \int_{-\infty}^{\infty} R(\tau) e^{-i\omega\tau} d\tau, \quad (2)$$

Table 1. Hydraulic Conditions and Characteristics of Temporal Series of Bed Elevation^a

Q_w (L/s)	D (m)	v (m/s)	S_w	h_R (m)	Shields Stress (τ_b^*)	Re	F_r	T_{mean} ($^{\circ}\text{C}$)	D_p (cm)	σ_b (mm)	k
2000	0.55	1.18	0.0019	0.39	0.058	646640	0.51	23.5	12.59	23.95	5.3
2800	0.64	1.55	0.0029	0.44	0.099	992000	0.62	16.23	19.17	38.65	5.0

^a Q_w , water discharge for the run; D , average depth of flow in test section; v , average flow velocity; h_R , hydraulic radius; S_w , water surface slope; τ_b^* , dimensionless Shields stress (computed using hydraulic radius); Re , Reynolds number (kinematic viscosity of water, $1 \times 10^{-6} \text{ m}^2/\text{s}$); F_r , Froude number; T_{mean} , mean water temperature; D_p , distance of the velocity probe from mean bed level; σ_b , standard deviation of temporal bed elevation series; and k , ratio between D_p and σ_b .

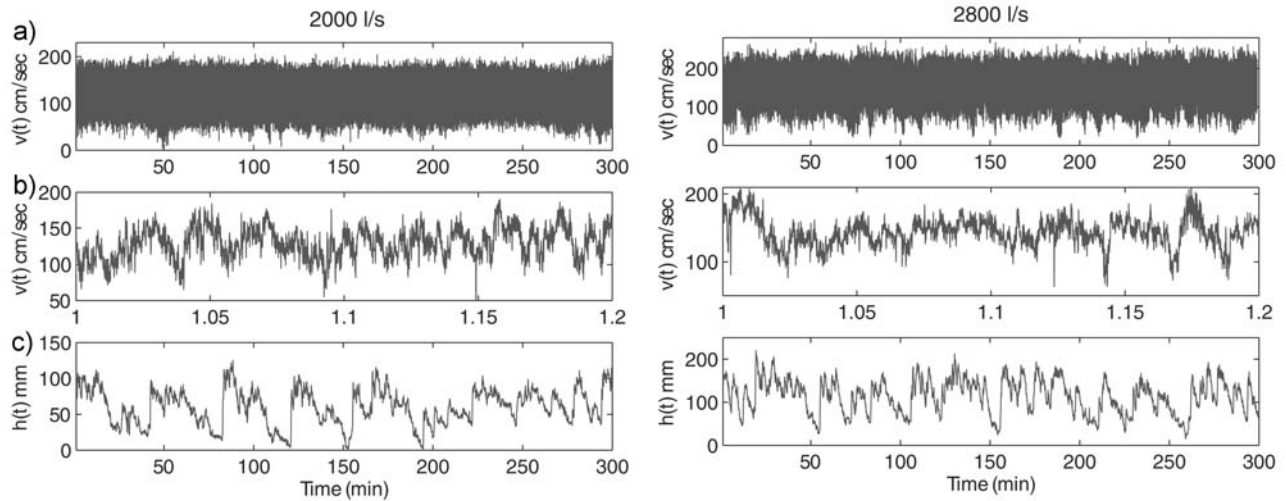


Figure 4. Time series of (a) velocity, (b) a blown-up image of the velocity series, and (c) bed elevation measured at the downstream end of the channel for a duration of 0.2 min for flow discharges of (left) 2000 L/s and (right) 2800 L/s over a duration of 300 min. The flow velocity was measured at a frequency of 200 Hz (sampling interval $\Delta t = 0.005$ s), and the bed elevations were sampled at a frequency of 0.2 Hz (sampling interval $\Delta t = 5$ s). In the case of bed elevation, it can be seen that short fluctuations are superimposed on larger ones. This suggests that small bed forms (small dunes, ripples, or bed load sheets) are propagated over larger dunes.

where $R(\tau)$ is the autocorrelation function defined as

$$R(\tau) = \frac{E[(X(t) - \mu)(X(t + \tau) - \mu)]}{\sigma^2}, \quad (3)$$

where τ is the time lag, μ and σ are the mean and standard deviation of the signal, respectively, and ω is the frequency. A simple way to estimate PSD is by taking the fast Fourier transform (FFT) of the signal [Stoica and Moses, 1997; Lacey and Roy, 2007]. In our case, the signal $X(t)$ is the flow velocity or the bed elevation in the streamwise direction. Special emphasis is placed here on identifying spectral scaling regimes, i.e., ranges of scales over which log-log linearity is observed in the power spectral density. (Note that the units for the velocity spectrum is quantity²/frequency, i.e., m²/s.)

[15] The power spectrum of the velocity fluctuations (measured at 200 Hz) at a discharge of 2000 L/s is shown in Figure 5a. Two clear scaling ranges can be observed, separated by a spectral gap. For relatively small scales (high frequencies) in the range of 0.1 s to 0.5 s, the slope of the PSD (power spectral density) is $\sim -5/3$, which corresponds to the inertial subrange of turbulence. A second scaling range is observed for scales between 2 min and 55 min, for which the slope of PSD is ~ -1.05 . The range of observed spectral gap is from 10 s to 2 min (see Table 2). The scales from the high-frequency end of the spectral gap which also coincides with the integral scale of the turbulence (see section 4 for discussion about ~ -1 spectral slope) to the low-frequency end of the inertial subrange shows a spectral slope ~ -1 . Figure 5b shows the PSD of the bed elevation (measured at sampling intervals of 5 s). A clear scaling is also found in the elevation field, with a PSD slope of ~ -1.94 for the scales of 15 s to 42 min (Table 2). Figures 6a and 6b show the power spectral density of the velocity fluctuations (measured at 200 Hz) and the bed elevations (measured at

0.2 Hz), respectively, for the discharge of 2800 L/s. The second scaling range (low-frequency regime) in the PSD of velocity fluctuations at the discharge of 2800 L/s is shifted toward higher frequencies and is from 35 s to 28 min with a spectral slope ~ -1.15 (Figure 6a). Temporal bed elevations for the same discharge show a scaling range of 15 s to 28 min with a spectral slope of -2.1 (Figure 6b). Figures 7a and 8a show the spatial bed transects for the discharge of 2000 L/s and 2800 L/s, respectively, measured along the centerline of the channel. The spectral slopes of spatial bed elevations are similar to those of temporal bed elevations as can be seen by comparison of Figures 5b and 7b and Figures 6b and 8b.

4. Interpretation of the Results and Discussion

[16] Power spectral densities of streamwise velocity have been studied extensively in the case of wall-bounded turbulent flows over flat homogeneous surfaces [e.g., Perry *et al.*, 1986; Katul *et al.*, 1995; Porté-Agel *et al.*, 2000]. In those flows, three scaling subranges have been identified. At low frequencies, a scaling subrange often referred to as the production subrange is found at scales larger than approximately $2\pi z$ (where z is the distance to the surface) and smaller than the integral scale of the turbulence (on the order of the depth of the flow in a channel). This range is characterized by a -1 spectral slope [Kader and Yaglom, 1991; Katul *et al.*, 1995]. At intermediate frequencies, an inertial subrange with a $-5/3$ spectral slope [Kolmogorov, 1961] is observed. It is associated with eddy scales smaller than approximately $2\pi z$. The third scaling subrange is the viscous subrange observed at smaller scales than the surface roughness size where spectra decays much faster than in the inertial subrange [Nezu and Nakagawa, 1993; Nikora and Goring, 2000].

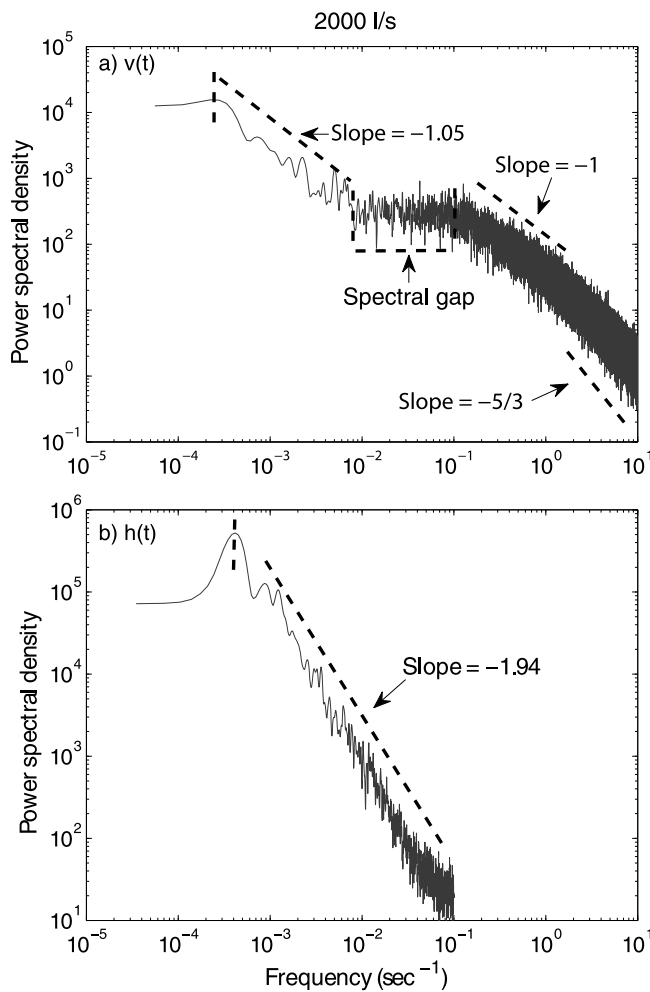


Figure 5. Power spectral density of (a) velocity fluctuations and (b) corresponding bed elevations for a discharge of 2000 L/s. In the velocity spectrum, scaling at small scales is due to turbulence, while at larger scales it is modulated by bed topography.

[17] In the case of flow over bed forms, it is expected that the turbulence will lead to similar scaling regimes as those found in the velocity spectra calculated over flat surfaces. More specifically, one would expect to find both an inertial subrange and a production subrange, even though the transition scale between these two ranges and the slope of the production subrange are likely to be affected by the presence of the topography, which may cause eddy shedding effects [Lapointe, 1992; Buffin-Bélanger and Roy, 1998; Hardy et al., 2007].

[18] In the hypothetical case of stationary bed forms, turbulence is the only source of velocity fluctuations and, consequently, no additional energy is introduced at scales

larger than the integral scale of the turbulence (on the order of the flow depth in the channel). However, in the case of a moving bed, the evolution of the bed forms introduces additional variability in the velocity field at the range of temporal scales associated with that evolution. We set forth the hypothesis that this effect explains the existence of the second scaling range (between 2 min and 55 min for the case of 2000 L/s, and 0.5 min to 28 min for the case of 2800 L/s) in the power spectrum of velocity, as shown in Figures 5a and 6a. Notice that the largest scale in that range (~55 min for 2000 L/s and 28 min for 2800 L/s) corresponds to the integral scale of the measured bed elevation field presented in Figures 5b and 6b. This largest scale is the characteristic time scale at which the largest bed forms move. Also notice that the second scaling range in the velocity spectra (scaling range due to bed form migration) shifts toward the higher frequencies, right in PSD, (compare Figure 5a to Figure 6a) with an increase in discharge, suggesting that the bed forms at higher flow (2800 L/s) are moving faster than the bed forms in the lower flow (2000 L/s). The clear signature of the large-scale bed forms on the multiscale variability of the velocity time series as captured in its PSD suggests the potential of using relatively low frequency velocity measurements near the bed to detect the characteristic time scales associated with the evolution of bed topography. The spectral analysis of our velocity measurements also shows that this scaling range is separated from the turbulence range by a spectral gap, i.e., a range of scales with virtually no additional contribution to the velocity variance.

[19] We hypothesize that the presence of a spectral gap is due to the lack of physical processes which could support the velocity fluctuations in this frequency range. A similar spectral gap was reported in the seminal work of Van Der Hoven [1957], who analyzed velocity time series collected in the atmospheric boundary layer. (Note that in that study the spectral density is plotted as $\omega S(\omega)$, while in our work it is $S(\omega)$.) In that flow, the gap separates the energy contributions associated with turbulence at the high frequencies from those corresponding to relatively slower frequency mesoscale and diurnal cycle variability. The presence of this gap has important practical implications since it allows to separate the contribution of the turbulence from that of mesoscale motions to the total kinetic energy and fluxes. Similarly, the presence of the spectral gap in channel flows with moving bed forms should be considered when using velocity time series to study turbulent transport in these flows.

[20] The high-frequency end of the spectral gap coincides with the integral scale of the turbulence, i.e., the scale of the largest turbulent eddies present in the flow. (Note that integral scale of turbulence is computed via visual inspection from Figures 5a and 6a of velocity spectra.) In Figures 5a and 6a, that integral scale is found at a frequency of

Table 2. Characteristics of Power Spectrum for Velocity, Temporal Bed Elevations, and Spatial Bed Elevations

Q_w (L/s)	Velocity $v(t)$			Temporal Bed Elevation $h(t)$		Spatial Bed Elevation $h(x)$	
	Dynamic Slope	Scaling Regime	Spectral Gap	Spectral Slope	Scaling Regime	Spectral Slope	Scaling Regime
2000	-1.05	2–55 min	10 s to 2 min	-1.94	15 s to 42 min	-1.87	10 cm to 10 m
2800	-1.15	35 s to 28 min	6–35 s	-2.1	15 s to 28 min	-2.06	15 cm to 10 m

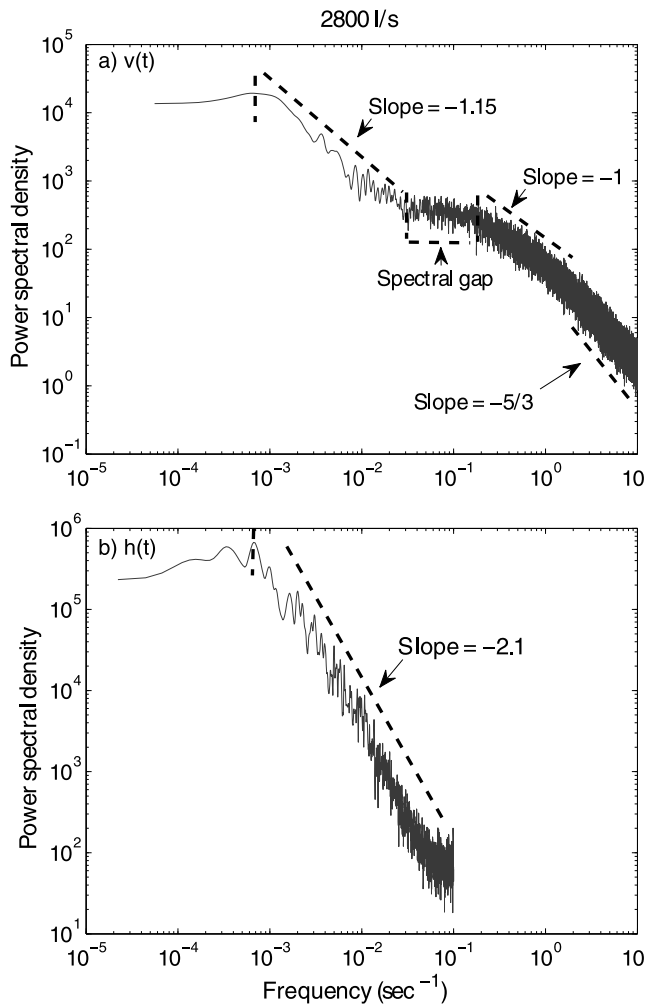


Figure 6. Power spectral density of (a) velocity fluctuations and (b) corresponding bed elevation for a discharge of 2800 L/s. In the velocity spectrum, scaling at small scales is due to turbulence, while at larger scales it is modulated by bed topography.

approximately 0.1 Hz for both flow discharges under consideration. The low-frequency end of the spectral gap is associated with the characteristic time scale of the smallest bed form structures that can be identified by the velocity sensor. From Figures 5a and 6a, that limit corresponds to frequencies of approximately 0.01 Hz and 0.02 Hz, for the 2000 L/s and 2800 L/s cases, respectively. This contrasts with the approximately 0.1 Hz associated with the relatively fast evolution of the smallest bed form structures, as shown in the spectral density of bed elevation (Figures 5b and 6b).

[21] It is important to note that the size of the smallest features detected by the velocity sensor and, as a result, the width of the spectral gap, should depend on the distance from the sensor to the bed. This is consistent with results from a previous study of the multiscale wavelet correlation between surface shear stress and velocity in a flat turbulent boundary layer [Venugopal *et al.*, 2003]. That study showed that turbulent eddies of vertical size smaller than the distance to the surface z (and horizontal size smaller than $2\pi z$) that affect the surface shear stress do not produce a signature

on the velocity measured at height z . With that in mind, here we speculate that the larger the distance between the velocity sensor and the surface, the larger the spectral gap. In general, the width of the spectral gap Δ_{gap} could be expressed as

$$\Delta_{gap} = f(k, \tau_b^*), \quad (4)$$

where $k = \frac{D_p}{\sigma_b}$, D_p is the distance from the probe to the mean bed level, and σ_b is the standard deviation of the temporal bed elevation (note that in our case, for both discharges, the ratio k is constant and close to 5). In the limiting case of a deep flow (flow depth much larger than bed form variability), if the velocity sensor is placed far enough from the bed surface, above the blending height (level above which the effect of the bed surface heterogeneity cannot be detected), the spectral gap would not exist. Future research will investigate this issue through comparison of spectra from measurements collected at different distances from the bed surface and, consequently, different k ratios.

[22] Bed elevation fields and their evolution are found to share important similarities with other natural surfaces such as landscapes. Landscapes present multiscale self-similar properties through a wide range of scales [see *Vening Meinesz*, 1951; *Newman and Turcotte*, 1990; *Pelletier*, 1999; *Passalacqua et al.*, 2006, and references therein]. In fact, *Passalacqua et al.* [2006] documented that landscapes also

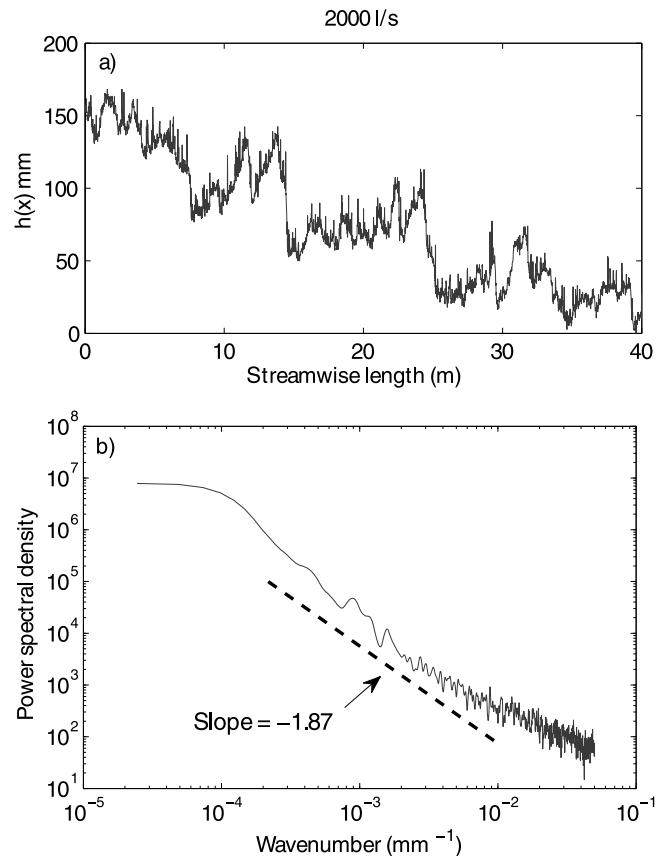


Figure 7. (a) Longitudinal transect of bed profile elevations at a resolution of 10 mm and (b) its power spectral density for a discharge of 2000 L/s. Note that similar spectral slopes are observed in both temporal bed elevation and spatial bed elevation series (compare with Figure 5b).

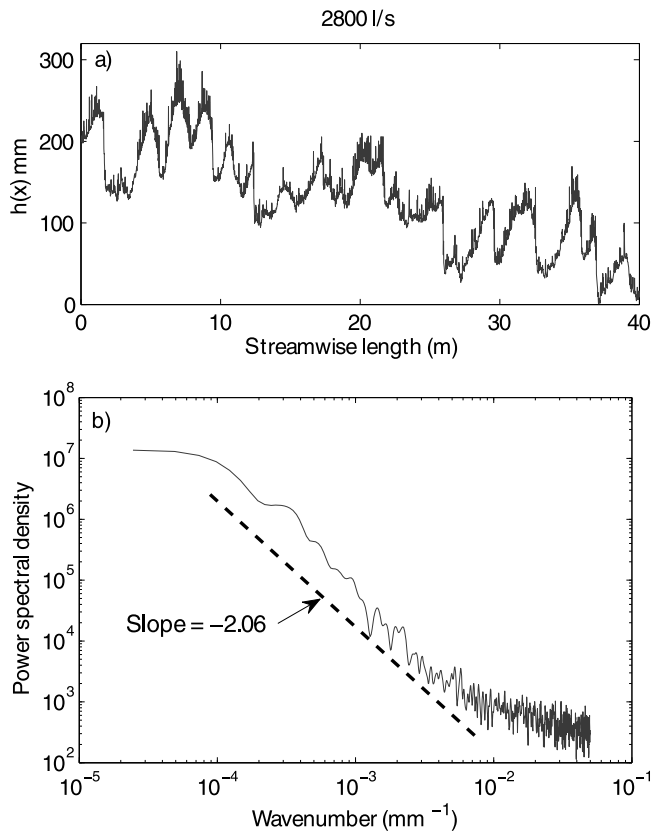


Figure 8. (a) Longitudinal transect of bed elevations sampled at a resolution of 10 mm and (b) its power spectral density for a discharge of 2800 L/s. Note that similar spectral slopes are observed in both temporal bed elevation and spatial bed elevation series (compare with Figure 6b).

share important similarities with turbulence since both systems exhibit scale invariance (self-similarity) over a wide range of scales and their behavior can be described using comparable dynamic equations. This similarity can be seen, for example, in the behavior of power spectra of the landscapes which exhibit a log-log scaling range with a slope of approximately -2 . Here also, we observe a slope of ~ -2 in power spectra of bed elevations for both the discharges of 2000 L/s and 2800 L/s (Figures 5b and 6b). Furthermore, *Singh et al.* [2009b] have shown the multiscale behavior of bed elevations (bed topography) for different flow conditions in a gravel bedded environment. In that study, they quantified the slope of the second-order structure function $2H$ (which is related to slope of the PSD with a relation $\beta = 2H + 1$, where β is the slope of PSD, and H is the Hurst exponent), and found that it is similar to the slope obtained here in the PSD of bed elevation fluctuations (Figures 5b and 6b). In the case of bed forms in gravel bedded channels little is known about the scaling properties of bed surfaces [*Nikora et al.*, 1998; *Marion et al.*, 2003; *Nikora and Walsh*, 2004]. For instance, *Nikora et al.* [1998] characterized gravel bed roughness using second-order structure functions. They found that the bed elevation distribution in laboratory flumes (unworked beds) and in natural gravel bed streams (water-worked beds) was close to Gaussian although the latter was skewed positively. They also observed that the scaling exponent (Hurst expo-

nent) $H = 0.79$ for natural beds was significantly higher than that of unworked beds, $H = 0.5$. A similar analysis was performed by *Aberle and Nikora* [2006].

[23] Spectral densities of the time series (Figures 5b and 6b) and of spatial transects (Figures 7b and 8b) of bed elevations are not independent of each other. Both have a clear scaling range with slope of approximately -2 , expanding over a similar range of scales (about two decades). The spatial spectra of bed elevation saturate at the same scale for both flow conditions (see Figures 7b and 8b and Table 2). That scale is about 10 m and it can be interpreted as the integral scale, i.e., the characteristic scale of the largest bed forms. The temporal scales associated with these bed forms are approximately 55 min and 28 min for the 2000 L/s and 2800 L/s flows, respectively (Figures 5 and 6). Considering these integral spatial and temporal scales, it is possible to determine a characteristic travel speed of the largest bed forms. This advection velocity is approximately 14 m/h and 22 m/h for the 2000 L/s and 2800 L/s discharges, respectively.

[24] Comparison of spectral densities of flow velocity and bed elevation measurements shows that relatively low resolution velocity measurements collected near the channel bed can be used to estimate the travel time of the largest bed forms. This application can potentially be used in the field; though it would require a long time series of river flow velocities [*Soulsby*, 1980; *Nikora and Goring*, 2000].

[25] Two major priorities for further research are suggested by this work. First, a better understanding is needed of what controls the slope of low-frequency velocity fluctuations in the PSD, and how it is related to the slope of PSD of temporal bed elevations and flow conditions. Second, the quantification of the dependence of length scale of the spectral gap on the Shields stress, depth-wise position of velocity measurements, and grain size distribution of the bed material should be undertaken. In order to meet these objectives, future work will be focused on the behavior of spectral density of velocity measured at different positions along the depth of the flow as a function of varying Shields stress and grain size distribution.

5. Conclusions

[26] This paper investigates the behavior of power spectral density of flow velocity and bed elevation time series measured in a large-scale experimental channel under two flow conditions. The power spectral density of the velocity shows two distinct power law scaling regimes. At high frequencies, an inertial subrange with $\sim -5/3$ Kolmogorov scaling is observed. It is associated with turbulent eddy motions of sizes smaller than the distance from the velocity sensor to the gravel bed. For slightly larger eddy scales, up to the integral scale of the flow, the effect of the bed leads to a reduction in the slope of the velocity spectrum. At lower frequencies, another scaling range with spectral slope of approximately -1.1 is found. This range is associated with the relatively slow evolution of the multiscale bed topography. At intermediate scales, a clear spectral gap, i.e., a range of scales with no additional energy contribution, separates the turbulence and bed evolution spectral ranges. The high-frequency limit of the spectral gap corresponds to the integral scale of the turbulence. The low-frequency end

of the gap corresponds to the scale of the smallest bed forms identified by the velocity sensor, and it is expected to depend on measurement location and bed variability. Our results also show that the temporal scales of the largest bed forms can be potentially identified from spectral analysis of low-resolution velocity measurements collected near the channel bed.

[27] **Acknowledgments.** This research was supported by the National Center for Earth-surface Dynamics (NCED), a Science and Technology Center funded by NSF under agreement EAR-0120914 as well as by NSF grants EAR-0824084 and EAR-0835789. Efi Foufoula-Georgiou gratefully acknowledges the support of the Ling Professorship Chair in Environmental Engineering. The experiments performed for this study are the followup of previous experiments (known as StreamLab06) conducted at the St. Anthony Falls Laboratory as part of an NCED program to examine physical-biological aspects of sediment transport (<http://www.nced.umn.edu>). We thank Jeff Marr, Craig Hill, and Sara Johnson for providing help in running the experiments. We also thank André Roy and two anonymous reviewers, as well as Christophe Ancely (Associate Editor), whose suggestions and constructive comments substantially improved our presentation and refined our interpretations. Computer resources were provided by the Minnesota Supercomputing Institute, Digital Technology Center at the University of Minnesota.

References

- Aberle, J., and V. Nikora (2006), Statistical properties of armored gravel bed surfaces, *Water Resour. Res.*, *42*, W11414, doi:10.1029/2005WR004674.
- Adrian, R. J., and C. S. Yao (1987), Power spectra of fluid velocities measured by laser Doppler velocimetry, *Exp. Fluids*, *5*, 117–128.
- Best, J. L. (1993), On the interactions between turbulent flow structure, sediment transport and bedform development: Some considerations from recent experimental research, in *Turbulence: Perspectives on Flow and Sediment Transport*, edited by N. J. Clifford, J. R. French, and J. Hardisty, pp. 61–92, John Wiley, Chichester, U. K.
- Buffin-Bélanger, T., and A. G. Roy (1998), Effects of a pebble cluster on the turbulent structure of a depth-limited flow in a gravel-bed river, *Geomorphology*, *25*, 249–267, doi:10.1016/S0169-555X(98)00062-2.
- Buffington, J. M., and D. R. Montgomery (1997), A systematic study of eight decades of incipient motion studies, with special reference to gravel-bedded rivers, *Water Resour. Res.*, *33*(8), 1993–2029.
- Dinehart, R. L. (1989), Dune migration in a steep, coarse-bedded stream, *Water Resour. Res.*, *25*(5), 911–923.
- Dinehart, R. L. (1992), Evolution of coarse gravel bedforms: Field measurements at flood stage, *Water Resour. Res.*, *28*(10), 2667–2689.
- Dinehart, R. L. (1999), Correlative velocity fluctuations over a gravel river bed, *Water Resour. Res.*, *35*(2), 569–582.
- Drake, T., R. Shreve, W. Dietrich, P. Whiting, and L. Leopold (1988), Bed-load transport of fine gravel observed by motion-picture photography, *J. Fluid Mech.*, *192*, 193–217.
- Fiedler, F., and H. A. Panofsky (1970), Atmospheric scales and spectral gaps, *Bull. Am. Meteorol. Soc.*, *51*, 1114–1119.
- Goring, D. G., and V. I. Nikora (2002), Despiking acoustic Doppler velocimeter data, *J. Hydraul. Eng.*, *128*(1), 117–126.
- Hardy, R. J., S. N. Lane, R. I. Ferguson, and D. R. Parsons (2007), Emergence of coherent flow structures over a gravel surface: A numerical experiment, *Water Resour. Res.*, *43*, W03422, doi:10.1029/2006WR004936.
- Hardy, R. J., J. L. Best, S. N. Lane, and P. E. Carbonneau (2009), Coherent flow structures in a depth-limited flow over a gravel surface: The role of near-bed turbulence and influence of Reynolds number, *J. Geophys. Res.*, *114*, F01003, doi:10.1029/2007JF000970.
- Hess, G. D., and R. H. Clarke (1973), Time spectra and cross-spectra of kinetic energy in the planetary boundary layer, *Q. J. R. Meteorol. Soc.*, *99*, 130–153.
- Imamoto, H., and T. Ishigaki (1986a), The three dimensional structure of turbulent shear flow in an open channel, paper presented at Fifth Congress, Asian and Pac. Reg. Div., Int. Assoc. for Hydraul. Res., Seoul.
- Imamoto, H., and T. Ishigaki (1986b), Visualization of longitudinal eddies in an open channel flow, in *Flow Visualization IV: Proceedings of the Fourth International Symposium on Flow Visualization*, edited by C. Veret, pp. 333–337, Hemisphere, Washington, D. C.
- Kader, B. A., and A. M. Yaglom (1991), Spectra and correlation functions of surface layer atmospheric turbulence in unstable thermal stratification, in *Turbulence and Coherent Structures*, edited by O. Métais and M. Lesieur, pp. 387–412, Kluwer Acad., Dordrecht, Netherlands.
- Katul, G. G., C. R. Chu, M. B. Parlange, J. D. Albertson, and T. A. Ortenburger (1995), Low wavenumber spectral characteristics of velocity and temperature in the atmospheric boundary layer, *J. Geophys. Res.*, *100*, 14,243–14,255.
- Kirkbride, A. D. (1993), Observations of the influence of bed roughness on turbulence structure in depth-limited flows over gravel beds, in *Turbulence: Perspectives on Flow and Sediment Transport*, edited by N. J. Clifford, J. R. French, and J. Hardisty, pp. 185–196, John Wiley, Chichester, U. K.
- Kirkbride, A. D., and R. I. Ferguson (1995), Turbulent flow structure in a gravel-bed river: Markov chain analysis of the fluctuating velocity profile, *Earth Surf. Processes Landforms*, *20*, 721–733.
- Kirkbride, A. D., and M. J. McLelland (1994), Visualization of the turbulent flow structures in a gravel bed river, *Earth Surf. Processes Landforms*, *19*, 819–825.
- Kolmogorov, A. (1961), Dissipation of energy in the locally isotropic turbulence, in *Turbulence: Classic Papers on Statistical Theory*, edited by S. K. Friedlander and L. Topper, pp. 151–155, Wiley Intersci., Hoboken, N. J.
- Lacey, R. W. J., and A. G. Roy (2007), A comparative study of the turbulent flow field with and without a pebble cluster in a gravel bed river, *Water Resour. Res.*, *43*, W05502, doi:10.1029/2006WR005027.
- Lacey, R. W. J., and A. G. Roy (2008), Fine-scale characterization of the turbulent shear layer of an instream pebble cluster, *J. Hydraul. Eng.*, *134*(7), 925–936.
- Lamarre, H., and A. G. Roy (2005), Reach scale variability of turbulent flow characteristics in a gravel-bed river, *Geomorphology*, *60*, 95–113.
- Lapointe, M. F. (1992), Burst-like sediment suspension events in a sand bed river, *Earth Surf. Processes Landforms*, *17*, 253–270.
- Marion, A., S. J. Tait, and I. K. McEwan (2003), Analysis of small-scale gravel bed topography during armoring, *Water Resour. Res.*, *39*(12), 1334, doi:10.1029/2003WR002367.
- Marquis, G. A., and A. G. Roy (2006), Effect of flow depth and velocity on the scales of macroturbulent structures in gravel-bed rivers, *Geophys. Res. Lett.*, *33*, L24406, doi:10.1029/2006GL028420.
- Newman, W. I., and D. L. Turcotte (1990), Cascade model for fluvial geomorphology, *Geophys. J. Int.*, *100*, 433–439.
- Nezu, I., and H. Nakagawa (1993), *Turbulence in Open-Channel Flows*, Balkema, Rotterdam, Netherlands.
- Nikora, V. (2008), Hydrodynamics of gravel-bed rivers: Scale issues, in *Gravel-Bed Rivers VI: From Process Understanding to River Restoration*, edited by H. Habersack, H. Piegay, and M. Rinaldi, pp. 61–81, Elsevier, New York.
- Nikora, V. I., and D. G. Goring (2000), Flow turbulence over fixed and weakly mobile gravel beds, *J. Hydraul. Eng.*, *126*(9), 679–690.
- Nikora, V., and J. Walsh (2004), Water-worked gravel surfaces: High-order structure functions at the particle scale, *Water Resour. Res.*, *40*, W12601, doi:10.1029/2004WR003346.
- Nikora, V. I., D. G. Goring, and B. J. F. Biggs (1998), On gravel-bed roughness characterization, *Water Resour. Res.*, *34*(3), 517–527.
- Paiement-Paradis, G., T. Buffin-Bélanger, and A. G. Roy (2003), Scalings for large turbulent flow structures in gravel-bed rivers, *Geophys. Res. Lett.*, *30*(14), 1773, doi:10.1029/2003GL017553.
- Parsheh, M., F. Sotiropoulos, and F. Porté-Agel (2010), Estimation of power spectra of acoustic-Doppler velocimetry data contaminated with intermittent spikes, *J. Hydraul. Eng.*, in press.
- Passalacqua, P., F. Porté-Agel, E. Foufoula-Georgiou, C. Paola (2006), Application of dynamic subgrid-scale concepts from large-eddy simulation to modeling landscape evolution, *Water Resour. Res.*, *42*, W06D11, doi:10.1029/2006WR004879.
- Pelletier, J. D. (1999), The self-organization and scaling relationships of evolving river networks, *J. Geophys. Res.*, *104*, 7359–7375.
- Perry, A. E., S. Henbest, and M. S. Chong (1986), A theoretical and experimental study of wall turbulence, *J. Fluid Mech.*, *165*, 163–199.
- Porté-Agel, F., C. Meneveau, and M. B. Parlange (2000), A scale-dependent dynamic model for large-eddy simulation: Application to a neutral atmospheric boundary layer, *J. Fluid Mech.*, *415*, 216–284.
- Robert, A., A. G. Roy, and B. De Serres (1992), Changes in velocity profiles at roughness transitions in coarse-grained channels, *Sedimentology*, *39*, 725–735.
- Robert, A., A. G. Roy, and B. De Serres (1993), Spacetime correlations of velocity measurements at a roughness transition in a gravel-bed river, in

- Turbulence: Perspectives on Flow and Sediment Transport*, edited by N. J. Clifford, J. R. French, and J. Hardisty, pp. 167–183, John Wiley, Chichester, U. K.
- Roy, A. G., T. Buffin-Belanger, H. Lamarre, and A. D. Kirkbride (2004), Size, shape and dynamics of large-scale turbulent flow structures in a gravel-bed river, *J. Fluid Mech.*, *500*, 1–27.
- Schmeeckle, M. W., J. M. Nelson, and R. L. Shreve (2007), Forces on stationary particles in near-bed turbulent flows, *J. Geophys. Res.*, *112*, F02003, doi:10.1029/2006JF000536.
- Shvidchenko, A. B., and G. Pender (2001), Macroturbulent structure of open-channel flow over gravel beds, *Water Resour. Res.*, *37*(3), 709–719.
- Singh, A., S. Lanzoni, and E. Foufoula-Georgiou (2009a), Nonlinearity and complexity in gravel-bed dynamics, *Stochastic Environ. Res. Risk Assess.*, *23*(7), 967–975, doi:10.1007/S00477-008-0269-8.
- Singh, A., K. Fienberg, D. J. Jerolmack, J. Marr, and E. Foufoula-Georgiou (2009b), Experimental evidence for statistical scaling and intermittency in sediment transport rates, *J. Geophys. Res.*, *114*, F01025, doi:10.1029/2007JF000963.
- Smedman-Högström, A. S., and U. Högström (1975), Spectral gap in surface-layer measurements, *J. Atmos. Sci.*, *32*, 340–350.
- Soulsby, R. L. (1980), Selecting record length and digitization rate for near-bed turbulence measurements, *J. Phys. Oceanogr.*, *10*, 208–219.
- Stoica, P., and R. L. Moses (1997), *Introduction to Spectral Analysis*, Prentice Hall, Upper Saddle River, N. J.
- Van Der Hoven, I. (1957), Power spectrum of horizontal wind speed in the frequency range from 0.0007 to 900 cycles per hour, *J. Meteorol.*, *14*, 160–194.
- Vening Meinesz, F. A. (1951), A remarkable feature of the Earth's topography, *Proc. K. Ned. Akad. Wet., Ser. B. Palaeontol. Geol. Phys. Chem. Anthropol.*, *54*, 212–228.
- Venugopal, V., F. Porté-Agel, E. Foufoula-Georgiou, and M. Carper (2003), Multiscale interactions between surface shear stress and velocity in turbulent boundary layers, *J. Geophys. Res.*, *108*(D19), 4613, doi:10.1029/2002JD003025.
- Wiberg, P. L., and J. D. Smith (1991), Velocity distribution and bed roughness in high-gradient streams, *Water Resour. Res.*, *27*(5), 825–838.
- Wilcock, P. R., C. H. Orr, and J. D. G. Marr (2008), The need for full-scale experiments in river science, *Eos Trans. AGU*, *89*(1), 6, doi:10.1029/2008EO010003.
- Yalin, M. S. (1992), *River Mechanics*, 219 pp., Elsevier, New York.

E. Foufoula-Georgiou, F. Porté-Agel, and A. Singh, Department of Civil Engineering, St. Anthony Falls Laboratory, University of Minnesota, Minneapolis, MN 55414, USA. (fporte@umn.edu)